0026-895X/05/6802-439–446$20.00
MOLECULAR PHARMACOLOGY
Vol. 68, No. 2
10876/3044328
Mol Pharmacol 68:439–446, 2005
Printed in U.S.A.

Integrin Engagement Increases Histone H3 Acetylation and Reduces Histone H1 Association with DNA in Murine Lung Endothelial Cells

Jane L. Rose, Hong Huang, Scott F. Wray, and Dale G. Hoyt

Division of Pharmacology, The Ohio State University College of Pharmacy (J.L.R., H.H., S.F.W., D.G.H.), and the Dorothy M. Davis Heart and Lung Research Institute (D.G.H.), Columbus, Ohio

Received December 28, 2004; accepted May 17, 2005

ABSTRACT

Engagement of integrin cell adhesion receptors in mouse lung endothelial cells induces global sensitivity of DNA to nuclease digestion, reflecting alterations in chromatin structure. These structural changes may contribute to the antigenotoxic effects of integrin engagement in lung endothelium. Because histone acetylation and poly(ADP-ribosyl)ation modulate chromatin structure, we investigated the effects of β1 integrin engagement with antibody on these post-translational modifications and the presence of histones at discrete DNA sequences in the mouse lung endothelial cell genome using chromatin immunoprecipitation. Integrin engagement increased acetylation of core histone H3. The presence of acetylated histone H3 at intercellular adhesion molecule-1 (ICAM-1) and vascular cell adhesion molecule-1 (VCAM-1) promoters, and a nonpromoter sequence was also increased. As with integrin engagement, the histone deacetylase inhibitor trichostatin A caused global hypersensitivity of DNA to nuclease digestion and induced acetylation of histone H3 and its coimmunoprecipitation with VCAM-1 and ICAM-1 promoters and nonpromoter DNA. In contrast to acetyl-histone H3, the association of linker histone H1 with specific DNA sequences was either reduced or unaffected by integrin engagement and trichostatin A. Although integrin engagement and trichostatin A treatment did not affect histone H1 poly(ADP-ribosyl)ation, deletion of poly(ADP-ribose) polymerase-1 increased core histone H3 acetylation and increased its level at the iNOS promoter while decreasing the amount of histone H1. The results suggest that integrin engagement, as well as trichostatin A and PARP-1 deletion, regulate chromatin structure via core histone H3 acetylation and reduced linker histone H1-DNA association.

Integrins are a family of heterodimeric cell surface receptors composed of $\alpha\beta$ subunits that mediate adhesion of cells to each other, extracellular matrix, and other ligands. Integrins mediate signal transduction, and antibodies to specific subunits promote endothelial survival (Meredith et al., 1993; Aplin et al., 1998). Integrin signaling modulates DNA damage and anticancer drug action in various cell types (Buckley et al., 1999; Hazlehurst et al., 2001). Engagement of β1 integrins with antibodies or peptide ligands inhibited rapid DNA strand breakage caused by bleomycin in mouse lung endothelial cells (MLEC) (Hoyt et al., 1997; Jones et al., 2001). Integrins also inhibit DNA strand breaks caused by bacterial endotoxin and the topoisomerase inhibitor etoposide. This ability to inhibit DNA damage caused by numerous agents might be due to a common mechanism, such as an alteration in the nucleus or stimulation of DNA repair (Hoyt et al., 1996a,b). Engagement of β1 integrins indeed alters MLEC chromatin structure, as indicated by an induction of global hypersensitivity of DNA to exogenous nucleases (Jones et al., 2001; Huang et al., 2003).

DNA digestion by nucleases is restricted by DNA-protein interactions in chromatin. Chromatin includes nuclear DNA organized in compact packages with proteins. The fundamental repeating unit of chromatin is the nucleosome, which contains ~146 to 165 bp of DNA wrapped around histone proteins. The nucleosome consists of two each of the core histones H2A, H2B, H3, and H4. Linker histone H1 binds nucleosomes where the coil of DNA enters and exits the core particle, and it attaches to DNA between nucleosomes, offering further stabilization of the chromatin fibers (Hansen, 2002).

This work was supported by grant HL68054 from the National Heart, Lung, and Blood Institute.
Article, publication date, and citation information can be found at http://molpharm.aspetjournals.org.
doi:10.1124/mol.104.010876.

ABBREVIATIONS: MLEC, mouse lung endothelial cells; bp, base pair(s); PARP-1, poly(ADP-ribose) polymerase-1; TSA, trichostatin A; HRP, horseradish peroxidase; PBS, phosphate-buffered saline; TTBS, Tris-buffered saline/Tween 20; PCR, polymerase chain reaction; INOS, inducible nitric-oxide synthase; ISNT, in situ nick translation; ChIP, chromatin immunoprecipitation; ICAM-1, intercellular cell adhesion molecule-1; VCAM-1, vascular cell adhesion molecule-1.

Chromatin structure is regulated by post-translational modifications of histones and through chromatin remodeling complexes. Modifications of histones include acetylation, poly(ADP-ribosyl)ation, methylation, phosphorylation, ubiquitination, and biotinylation (Hansen, 2002). Acetylation of core histones and poly(ADP-ribosyl)ation of linker histone enhance digestibility of cellular DNA with nucleases (Simpson, 1978; Perez-Lamigueiro and Alvarez-Gonzalez, 2004).

Electrostatic effects of acetylation and poly(ADP-ribosyl)ation alter histone-DNA and histone-protein interactions in the nucleus, contributing to nuclease hypersensitivity. Acetylation of N-terminal tails of core histones neutralizes positive charge on lysines and disrupts interaction with negative phosphates in the backbone of DNA (Hansen, 2002). Poly(ADP-ribosyl)ation, largely mediated by poly(ADP-ribose) polymerase-1 (PARP-1), occurs mainly on linker histone H1. Negatively charged ADP-ribose polymers interact poorly with anionic DNA, increasing accessibility of proteins to DNA (D'Amours et al., 1999; Ame et al., 2004). These post-translational modifications may contribute to integrin-mediated alterations in chromatin.

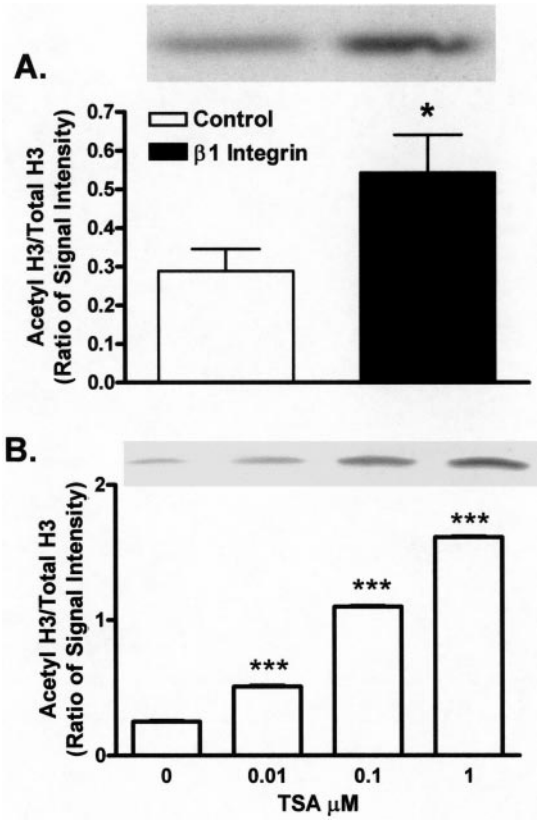

Fig. 1. Effect of integrin engagement and TSA on acetylation of core histones. A, MLEC were treated with 0 or 1 μg/ml β1 integrin antibody for 1 h and then with goat-anti rat IgG (2 μg/ml final concentration) for 4 h. Proteins were extracted and processed for Western blotting. Inset, representative image of acetyl-histone H3 in 0 or 1 μg/ml β1 integrin antibody treatments. B, MLEC were treated with 0, 0.01, 0.1, and 1 μM TSA for 24 h. Proteins were extracted and processed for Western blotting. Acetyl-histone H3 was measured by Western blotting and analyzed densitometrically. Blots were also probed with total histone H3 antibody, analyzed, and used to normalize acetyl-histone H3 levels. Bars represent the mean ± S.E. of four independent cultures per treatment group. *, $p < 0.05$ for comparison with 0 μg/ml β1 integrin antibody. ***, $p < 0.001$ for comparison with 0 μM TSA. Inset, representative image of acetyl-histone H3 in 0, 0.01, 0.1, or 1 μM TSA treatment.

Because acetylation and poly(ADP-ribosyl)ation regulate histone interactions with DNA and other proteins, we hypothesized that integrin-mediated nuclease hypersensitivity is due to one or both of these histone modifications. Integrin actions on acetylation of core histone H3 and poly(ADP-ribosyl)ation of linker histone H1 were measured and compared with the effect of raising histone acetylation with the histone deacetylase inhibitor trichostatin A (TSA) and with PARP-1 knockout. Colocalization of these histones with specific DNA sequences in the genome of live cells was assessed by chromatin immunoprecipitation (ChIP). The results suggest that integrin engagement, trichostatin A, and PARP-1 knockout each increase histone H3 acetylation and alter the association of histone H1 with DNA.

Materials and Methods

Reagents. Endothelial cell growth supplement, heparin, phenylmethylsulfonyl fluoride, goat anti-rat IgG, phenol-chloroform-isoamyl alcohol, and Bradford reagent were purchased from Sigma Chemical Co. (St Louis, MO). Fetal bovine serum was purchased from Hyclone Laboratories (Logan, UT). Rat anti-mouse β1 integrin antibody was from BD PharMingen (San Diego, CA). Mouse anti-histone H1, rabbit anti-histone H3, and rabbit anti-acetyl lysine 9 and 14 histone H3 were purchased from Upstate Biotechnologies Inc. (Charlottesville, VA). Rabbit anti-poly(ADP-ribose) was obtained from BIOMOL Research Laboratories, Inc. (Plymouth Meeting, PA). Mouse anti-PARP-1 C2–10 antibody was obtained from Trevigen Inc. (Gaithersburg, MD). Horseradish peroxidase (HRP)-conjugated goat anti-mouse and goat anti-rabbit were from Jackson ImmunoResearch Laboratories, Inc. (West Grove, PA). Gamma Bind Plus Sepharose was from Amersham Biosciences (Uppsala, Sweden). Bovine serum albumin and digoxigenin-11-dUTP were purchased from Roche Applied Science (Indianapolis, IN). DNA polymerase I was from New England Biolabs (Beverly, MA). Salmon sperm DNA, proteinase K, deoxynucleotides, platinum *Taq* DNA polymerase, DNase I, and trypsin were purchased from Invitrogen (Carlsbad, CA). Tris-base, sodium chloride, EDTA, Na_3VO_4, NaF, Tween 20, formaldehyde, SDS, agarose, and ethidium bromide were from Fisher Scientific (Fair Lawn, NJ). Triton X-100 was purchased from Pierce (Rockford, IL).

Cell Culture. Murine lung microvascular endothelial cells (MLEC) were isolated from wild-type (+/+) and PARP-1 knockout (−/−) mice as described previously (Jones et al., 2001).

Treatment of Cells. Integrin engagement with anti-β1 Integrin antibody was performed as described previously (Hoyt et al., 1996a,b). PARP-1 +/+ and −/− MLEC were plated onto 75-cm^2

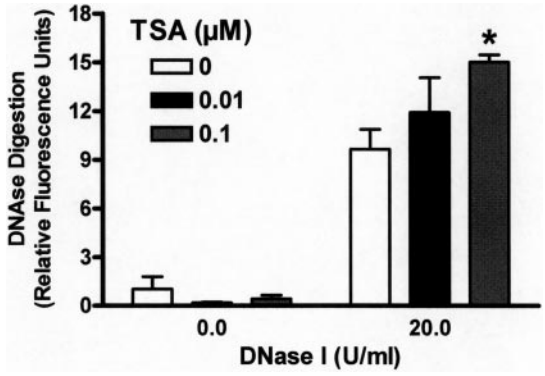

Fig. 2. Effect of TSA on DNase I sensitivity. MLEC were treated with 0, 0.01, and 0.1 μM TSA for 24 h. Cells were processed and digested with 20 U/ml DNase I for 25 min, and breaks in DNA were labeled by ISNT. Bars represent the mean of fluorescence intensity ± S.E. of the difference for six wells for each experimental group. *, $p < 0.05$ for comparison between 0 and 0.1 μM TSA in DNase-treated wells.

flasks and, 24 h later, rinsed once with phosphate-buffered saline (PBS) and treated with 0 or 1 μg of anti-β1 integrin antibody/ml for 1 h at 37°C. Goat anti-rat IgG was added to all flasks for another 4 h of incubation at 37°C.

Cell Lysis. MLEC were washed three times with ice-cold PBS and lysed with lysis buffer containing 1% Triton X-100, 50 mM Tris, pH 7.5, 150 mM NaCl, 5 mM EDTA, 0.5 mM Na_3VO_4, 50 mM NaF, 10 μg/ml aprotinin, 10 μg/ml leupeptin, 10 μg/ml pepstatin A, and 1 mM phenylmethylsulfonyl fluoride. Extracts were sonicated, and protein concentration was determined by the Bradford assay.

Immunoprecipitation. For immunoprecipitation of histone H1, 200 μg of protein was incubated with 2 μg of anti-histone H1 antibody overnight at 4°C. A 30% slurry of protein G Sepharose was added to each sample and rocked gently at 4°C for another 1 h. The antibody-antigen-Sepharose pellet was washed three times in ice-cold lysis buffer and two times in 10 mM Tris, pH 7.4. The washed pellet was reconstituted in protein loading buffer (62.5 mM Tris, pH 6.8, 10% glycerol, 2% SDS, 5% β-mercaptoethanol, and 0.003% bromphenol blue) and heated for 10 min at 95°C. Proteins were separated on a 4 to 20% Tris-glycine polyacrylamide gel.

Total Protein Preparation. For total protein analysis, 10 μg of protein was incubated with protein loading buffer and incubated for 10 min at 95°C. Proteins were separated on 4 to 20% Tris-glycine polyacrylamide gels.

Immunoblotting. After transfer, the blots were blocked with 3% nonfat dry milk in Tris-buffered saline buffer and Tween 20 (TTBS; 0.1% Tween 20, 10 mM Tris, pH 7.5, and 150 mM NaCl) and probed with primary antibody for 1 h at room temperature. After blots were washed, appropriate HRP-conjugated secondary antibody was added and incubated for 1 h. Proteins were visualized using enhanced chemiluminescent system and captured on X-ray film.

Chromatin Immunoprecipitation. After treatment, MLEC were fixed by addition of formaldehyde to a concentration of 1% directly in the culture medium for 10 min at 37°C. Cells were washed three times with PBS and scraped in ice-cold collecting buffer (PBS with 10 μg/ml leupeptin, 10 μg/ml aprotinin, 10 μg/ml pepstatin A, and 1 mM phenylmethanesulfonyl fluoride). Collected cells were centrifuged at 2000 rpm for 4 min at 4°C. Pellets were resuspended in ice-cold lysis buffer (1% SDS, 10 mM EDTA, and 50 mM Tris pH 8.1) and incubated on ice for 10 min. Chromatin was sheared to 1-kilobase fragments by sonication (four pulses, 20 s per pulse, at one-sixth maximum power) followed by addition of dilution buffer (0.01% SDS, 1.1% Triton X-100, 1.2 mM EDTA, 16.7 mM Tris, pH 8.1, and 167 mM NaCl). Immunoprecipitation of target histone protein was performed with the addition of 10 μg of anti-Histone H1 or 10 μg of anti-acetyl histone H3 (Lys 9 and 14) with gentle rocking overnight at 4°C. Immune complexes were collected for 1 h on Gamma Bind Plus Sepharose with 20 μg/ml salmon sperm DNA. Immune complexes were sequentially washed for 4 min on ice with

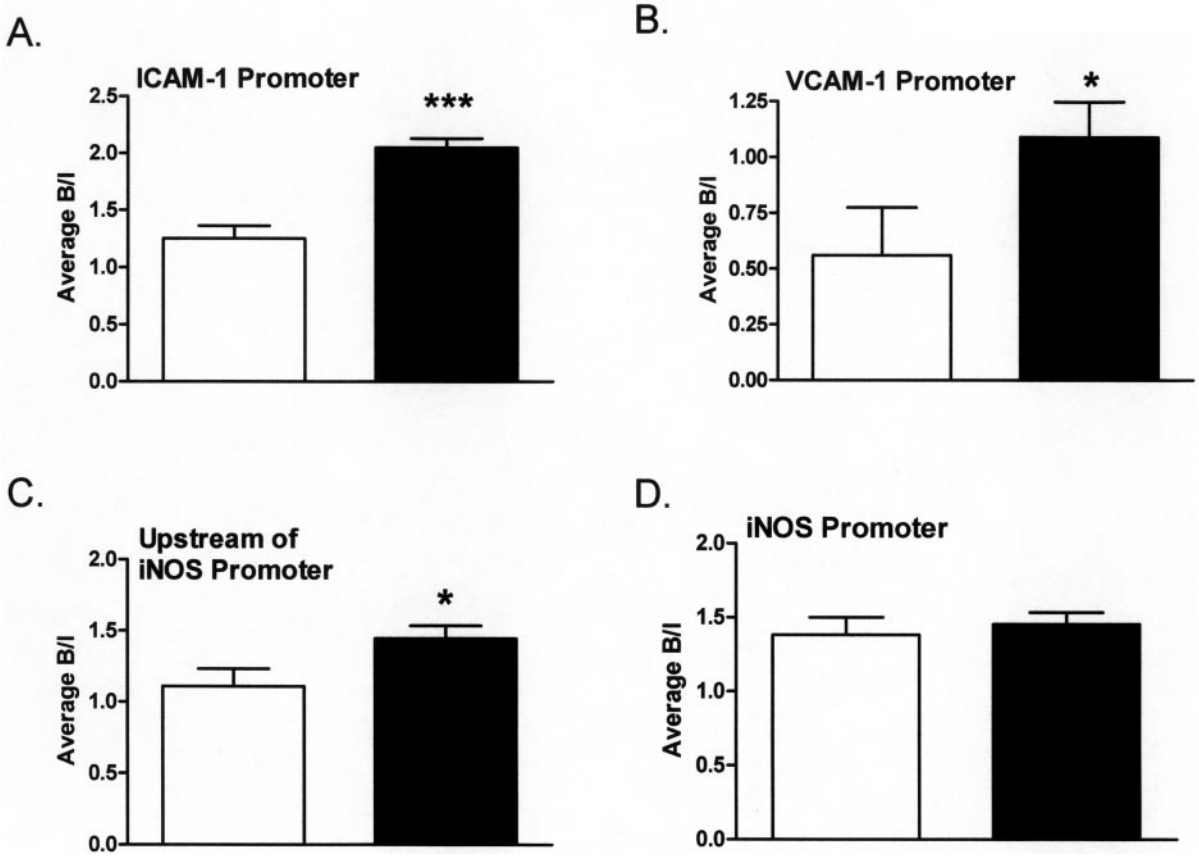

Fig. 3. Effect of integrin engagement on acetylation of histone H3 at local genomic sites using ChIP. MLEC were treated with 0 (□) or 1 μg/ml β1 integrin antibody for 1 h (■), and then with goat-anti rat IgG (2 μg/ml final concentration) for 4 h. Cells were treated with formaldehyde to cross-link proteins, proteins immunoprecipitated with 10 μg of anti-acetyl-histone H3 antibody, reverse cross-linked and associated DNA was isolated and amplified using PCR. Bars represent the average ± S.E. of bound (*B*) over input (*I*) levels analyzed densitometrically from 1% agarose gels from four independent cultures per treatment group with at least nine independent PCR reactions per treatment. The *B* level represents PCR product from samples immunoprecipitated with antibody with no antibody blank subtracted. *I* is the PCR product from 1% of the sample before immunoprecipitation used to normalize for treatment changes in total DNA content. A dilution series of template DNA was used to ensure PCR product formation increased linearly with template concentration. *, $p < 0.05$; ***, $p < 0.0001$ for comparison between 0 and 1 μg/ml β1 integrin antibody. A, acetyl-histone H3 coimmunoprecipitated with the ICAM-1 promoter. B, acetyl-histone H3 coimmunoprecipitated with the vascular adhesion molecule-1 (VCAM-1) promoter. C, acetyl-histone H3 coimmunoprecipitated with sequences upstream of the iNOS promoter. D, acetyl-histone H3 coimmunoprecipitated with the iNOS promoter.

elution buffer A (0.1% SDS, 2 mM EDTA, 20 mM Tris, pH 8, 150 mM NaCl, and 1% Triton X-100), elution buffer B (0.1% SDS, 2 mM EDTA, 20 mM Tris, pH 8, 500 mM NaCl, and 1% Triton X-100), elution buffer C (0.25 M LiCl, 1% Nonidet P-40, 1 mM EDTA, 10 mM Tris, pH 8, and 1% sodium deoxycholate), and two washes with 10 mM Tris and 1 mM EDTA, pH 8. Immune complexes were eluted with 1% SDS in 0.1 M $NaHCO_3$ and incubated at 65°C overnight to reverse DNA-protein cross-links. After proteinase K digestion (20 μg, 1 h, 45°C) DNA was recovered with phenol-chloroform-isoamyl alcohol extraction and precipitated in ethanol. DNA was resuspended in 13.5 μl of a mixture of 10 mM Tris and 1 mM EDTA and serially diluted to 1/12, 1/24, 1/48, and 1/96 of immunoprecipitated DNA for polymerase chain reactions (PCR) used to detect the relative level of specific DNA sequences recovered with the immunoprecipitated protein. Input samples (1% of volume after sonication) were reverse–cross-linked and processed in the same way as immunoprecipitated DNA. The following promoter specific primers were used. inducible nitric-oxide synthase (iNOS): sense, 5′-CAACTATTGAGGCCACACAC-3′; antisense, 5′-AACCAGTGACACTGTGTCC-3′; 1133-bp product. VCAM-1: sense, 5′-CATTCTGCATCAACGTCC-3′; antisense, 5′-AAGTACCGTTGAGGCTCC-3′; 830-bp product. ICAM-1: sense: 5′-CTTGGATCGCTGCTTCAT-3′; antisense, 5′-AGCGGAGCTCAGCACTA-3′; 592-bp product. As a probe of a non-promoter DNA, primers for a region upstream of the iNOS promoter were generated: sense, 5′-GTGTCACACCACAGAGCTGC-3′; antisense, 5′-GTGTCTCTGCTCCTCCATCC-3′; 984-bp product. The PCR conditions were as follows: 5 μl of 10× *Taq* buffer, 1.2 to 1.8 mM $MgCl_2$, 200 μM deoxyribonucleotides, 0.6 μM primer mix, 0.05 units of platinum *Taq* DNA polymerase and H_2O to a final volume of 50 μl. PCR conditions were as follows: 94°C for 90 s; 35 cycles at 94°C for 30 s, 54–66°C (depending on primer set) for 30 s and 72°C for 60 s; final elongation at 72°C 10 min. Samples were run on a 1% agarose gel and bands, digitally imaged, analyzed with Image J software (ver. 1.22d; http://rsb.info.nih.gov/ij/), and the integrated intensity of bands was calculated. The average pixel intensity and number of pixels in a band were multiplied to determine the total signal intensity. The ratio of antibody bound DNA samples was divided by the input sample for each dilution. The ratios were averaged for each treatment condition and indicate the relative presence of histones on specific DNA sequences.

DNase I Digestion and in Situ Nick Translation. After treatment of six wells per condition, cells in 96-well plates were fixed by addition of formaldehyde directly into the medium to a concentration of 1% for 10 min at 37°C. Cells were washed three times with PBS and made permeable by incubation overnight in 70% ethanol at −20°C. Cells were washed three times with PBS at 4°C. The relative sensitivity of nuclear DNA to digestion with exogenous nucleases was used to detect global alterations in chromatin structure (Hewish and Burgoyne, 1973; Hoyt et al., 1996a,b). Cells were rinsed in ISNT buffer (2.5 mM $MgCl_2$, 50 mM Tris, pH 7.8, 10 mM β-mercaptoethanol, and 10 μg/ml bovine serum albumin) and then digested for 25 min at room temperature with 0 or 20 units/ml DNase I in ISNT buffer. The cells were rinsed three times with PBS. DNA breaks were then labeled by ISNT with digoxigenin-dUTP (Hoyt et al., 1997). Cells were incubated at 37°C for 80 min with ISNT buffer containing 16 μM concentrations of dGTP, dATP, and dCTP, 16 μM digoxigenin-dUTP, and 2 U/ml DNA polymerase I. Labeling was stopped by rinsing with PBS. Wells were blocked with 10% goat serum/TTBS for 1 h, incubated for 1 h with a 1:1000 dilution of mouse anti-digoxigenin in 10% goat serum/TTBS, washed three times with TTBS, and

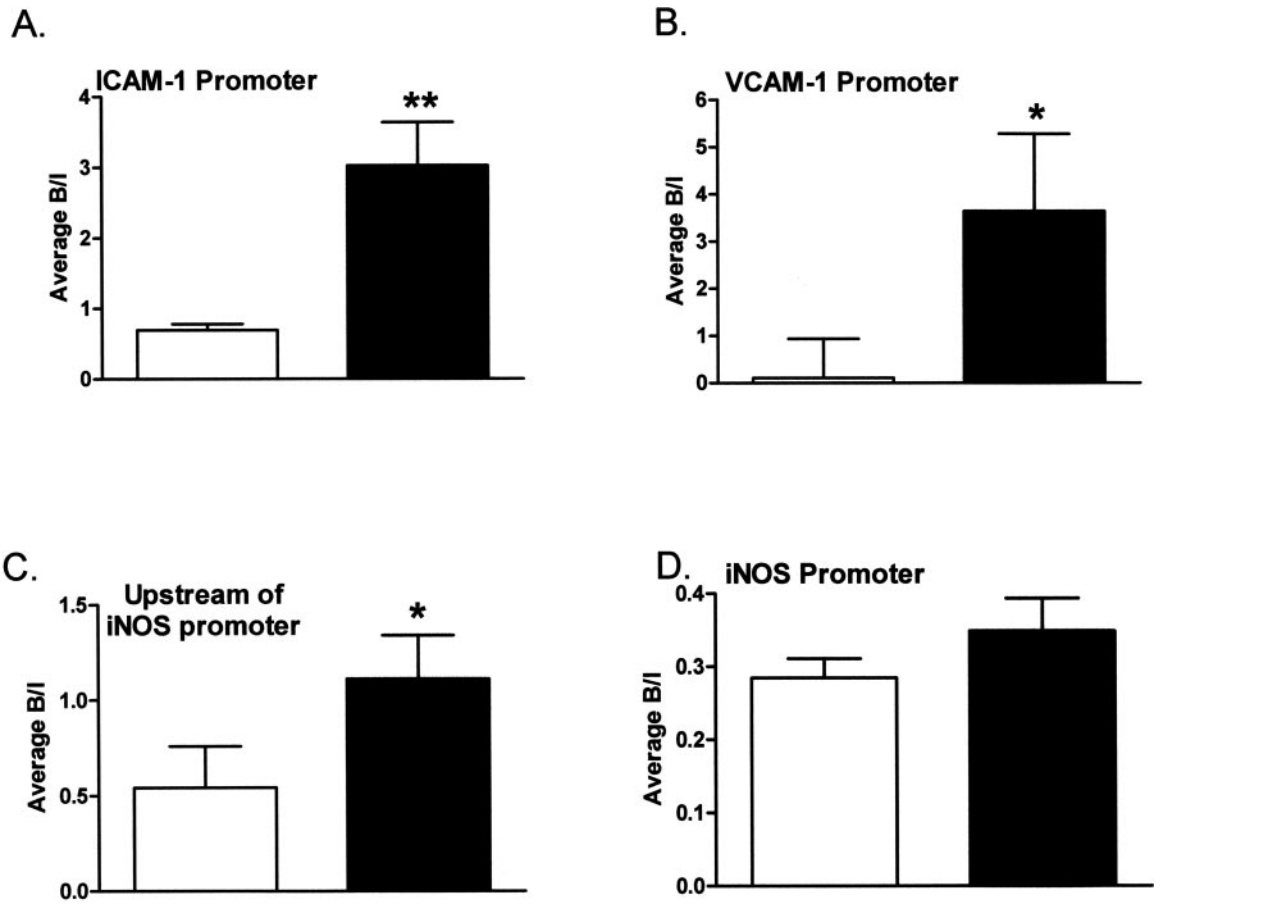

Fig. 4. Effect of TSA on acetylation of histone H3 at local genomic sites using ChIP. MLEC were treated with 0 (□) or 0.1 μM TSA (■) for 24 h. Cells were processed as in Fig. 3. A, acetyl-histone H3 coimmunoprecipitated with the ICAM-1 promoter. B, acetyl-histone H3 coimmunoprecipitated with the VCAM-1 promoter. C, acetyl-histone H3 coimmunoprecipitated with sequences upstream of the iNOS promoter. D, acetyl-histone H3 coimmunoprecipitated with the iNOS promoter. *, $p < 0.05$; **, $p < 0.001$ for comparison between 0 and 0.1 μM TSA.

incubated for 1 h with 1:1000 dilution of goat anti-mouse HRP antibody. Amplex red reagent and hydrogen peroxide were added to each well according to manufacturer's instructions (Molecular Probes, Eugene, OR). Fluorescence was detected in a fluorescent microplate reader with excitation at 562 nm, emission at 599 nm, and a cutoff at 590 nm. Relative fluorescence units were obtained at 15 min in the linear phase of fluorescence. DNA content in each well was determined by addition of 25 ug/ml 33342 Hoechst with excitation at 355 nm and emission at 465 nm. Relative fluorescence units were normalized to DNA content in each well.

Statistical Testing. Data were analyzed by Student's *t* test or by analysis of variance with Bonferroni correction for multiple comparisons (Snedecor and Cochrane, 1980).

Results

Previous studies demonstrated that engagement of β1 integrins with antibody caused a global increase in sensitivity of MLEC DNA to digestion with nucleases (Jones et al., 2001). To determine the mechanisms underlying nuclease hypersensitivity, specific components of the chromatin architecture were probed for distinct post-translational modifications. Poly(ADP-ribosyl)ation and acetylation generally cause decondensation of chromatin, rendering DNA more susceptible to digestion with nucleases (Simpson, 1978; Realini and Althaus, 1992).

Linker histone H1 is the predominant histone modified with poly(ADP-ribose), which relaxes chromatin. Furthermore, a role for PARP-1 in integrin action was suggested by observations that integrin engagement failed to inhibit drug-induced DNA breakage in PARP-1 knockout cells and that knockouts were hypersensitive to DNase I (Jones et al., 2001; Huang et al., 2003). Therefore, we assessed poly(ADP-ribosyl)ation of histone H1 and its association with PARP-1 and DNA by immunoprecipitation of histone H1 from wild-type and PARP-1 knockout MLEC. PARP-1 coimmunoprecipiated with histone H1 in untreated wild-type cells, reflecting a basal association between the two proteins, and trichostatin A and integrin engagement did not affect this interaction. Furthermore, poly(ADP-ribosyl)ation of PARP-1 and of histone H1 in H1 immunoprecipitates was unaffected by trichostatin A or integrin engagement (data not shown). Histone H1 levels in PARP-1 knockout MLEC were equal to those in wild-type cells and, as expected, no poly(ADP-ribosyl)ation or association of PARP-1 with histone H1 was detected in the knockouts (not shown). The results indicate that integrin engagement and trichostatin A did not affect poly(ADP-ribosyl)ation of the 2 main nuclear substrates of PARP-1.

We next measured the effect of integrin engagement on histone acetylation. Wild-type MLEC were treated with integrin antibody and proteins were extracted for Western blotting. Figure 1A demonstrates a significant increase in acetyl-histone H3 in β1 integrin antibody-treated MLEC.

The effect of raising histone acetylation with a broad-spectrum histone deacetylase inhibitor, trichostatin A, was compared with integrin engagement. As expected, trichostatin A caused a concentration-dependent increase in global acetylation of histone H3 (Fig. 1B). Trichostatin A also increased the sensitivity of nuclear DNA to digestion with DNase I (Fig. 2).

Chromatin immunoprecipitation was used to measure local alterations in histone-DNA colocalization in live cells. We determined the effect of integrin engagement on the level of acetyl-histone H3 at the ICAM-1, VCAM-1, and iNOS promoter DNA sequences, near the start codons of these genes, where specific transcription factors are known to bind. Histone coimmunoprecipitation with a region that was 4763 base pairs 5′ of the iNOS promoter sequence, which is characterized by a lack of consensus sites for transcription factors, was also measured. Integrin engagement increased the coimmunoprecipitation of acetyl-histone H3 with ICAM-1 and VCAM-1 promoters, and with the sequence upstream of the iNOS promoter (Fig. 3 A–C). There was no effect on acetyl-histone H3 coimmunoprecipitation with the iNOS promoter sequence (Fig. 3D).

Because integrin engagement increased global and local histone H3 acetylation, we next determined the effect of trichostatin A on acetyl-histone H3 chromatin immunoprecipitation. As seen with β1-integrin engagement, trichostatin A increased the level of acetyl-histone H3 coimmunoprecipitated with VCAM-1 and ICAM-1 promoters and with the iNOS upstream sequence (Fig. 4, A–C). Also as with integrin engagement, acetyl-histone H3 coimmunoprecipitated with iNOS promoter DNA was not affected by trichostatin A (Fig. 4D).

The effects of trichostatin A and integrin engagement on association of linker histone H1 with DNA was determined because reduced association of histone H1 with DNA may render DNA susceptible to nuclease digestion (Hansen, 2002). The histone H1 content of MLEC, measured by Western blotting, was not affected by β1-integrin antibody or trichostatin A (not shown). Integrin engagement decreased the level of linker histone H1 associated with the VCAM-1

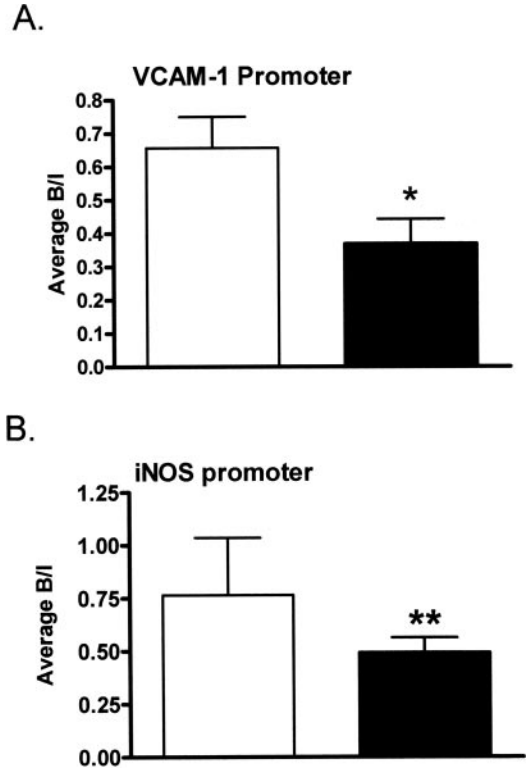

Fig. 5. Effect of integrin engagement on association of histone H1 at local genomic sites using ChIP. MLEC were treated with 0 (□) or 1 μg/ml β1 integrin antibody (■) for 1 h and then with goat-anti rat IgG (final concentration, 2 μg/ml) for 4 h. Cells were processed as in Fig. 3, except that 10 μg of histone H1 antibody was used for immunoprecipitation. A, histone H1 associated with the VCAM-1 promoter. B, histone H1 associated with the iNOS promoter. **, $p < 0.01$ for comparison between 0 and 1 μg/ml β1 integrin antibody.

and iNOS promoters (Fig. 5). Trichostatin A treatment reduced the association of histone H1 with the ICAM-1 and VCAM-1 promoters, and with the iNOS upstream sequence, but not with the iNOS promoter (Fig. 6).

Acetyl-histone H3 levels were greatly elevated in PARP-1 knockout relative to wild-type MLEC (Fig. 7). Furthermore, as with integrin engagement and treatment of wild-type cells with trichostatin A, coimmunoprecipitation of acetyl-histone H3 with VCAM-1 and iNOS promoter DNA and with DNA 5′ of the iNOS promoter was increased in knockouts (Fig. 8, B–D). In contrast, coimmunoprecipitation of ICAM-1 promoter DNA was reduced in PARP-1 knockout cells (Fig. 8A). As with integrin engagement and trichostatin A treatment, the amount of histone H1 at the iNOS promoter was decreased (Fig. 9). These data indicate that acetylation of the core histone H3 is increased in response to deletion of PARP-1 and that there were changes in histone-DNA coimmunoprecipitation that were generally similar, but not identical, to those caused by integrin engagement or the histone deacetylase inhibitor.

Discussion

We found previously that β1 integrin engagement increased the sensitivity of MLEC DNA to digestion by nucleases, indicating that chromatin structure is altered (Jones et al., 2001; Huang et al., 2003). In this study, we investigated the impact of integrin engagement on poly(ADP-ribosyl)ation and histone acetylation because both post-translational modifications regulate chromatin structure (Peterson and Cote, 2004).

Poly(ADP-ribosyl)ation of histones and other nuclear proteins dramatically increases negatively charged polymers of ADP-ribose in the vicinity of DNA breaks resulting in relaxation of chromatin structure (Perez-Lamigueiro and Alvarez-Gonzalez, 2004). This action of PARP-1 is thought to aid in the recruitment and access of DNA repair proteins to sites of DNA breaks (D'Amours et al., 1999; Parsons et al., 2005). We found previously that integrin-mediated suppression of bleomycin- and LPS-induced DNA strand breakage was prevented in PARP-1 knockout MLEC (Jones et al., 2001; Huang et al., 2003). Therefore, we hypothesized that integrin engagement might activate PARP-1 to generate polymers of ADP-ribose on nuclear proteins that would enhance nuclease sensitivity, recruit repair proteins, and ultimately suppress DNA damage. However, we found here that integrin engagement had no affect on poly(ADP-ribose) formation on the major PARP-1 targets, histone H1 and PARP-1. The requirement for PARP-1 in integrin-mediated suppression of drug-induced DNA breakage may be due to the direct role of PARP-1 protein in facilitating DNA repair rather than through modification of chromatin.

Acetylation of lysines neutralizes positive charge and reduces interaction of amino tails with negatively charged

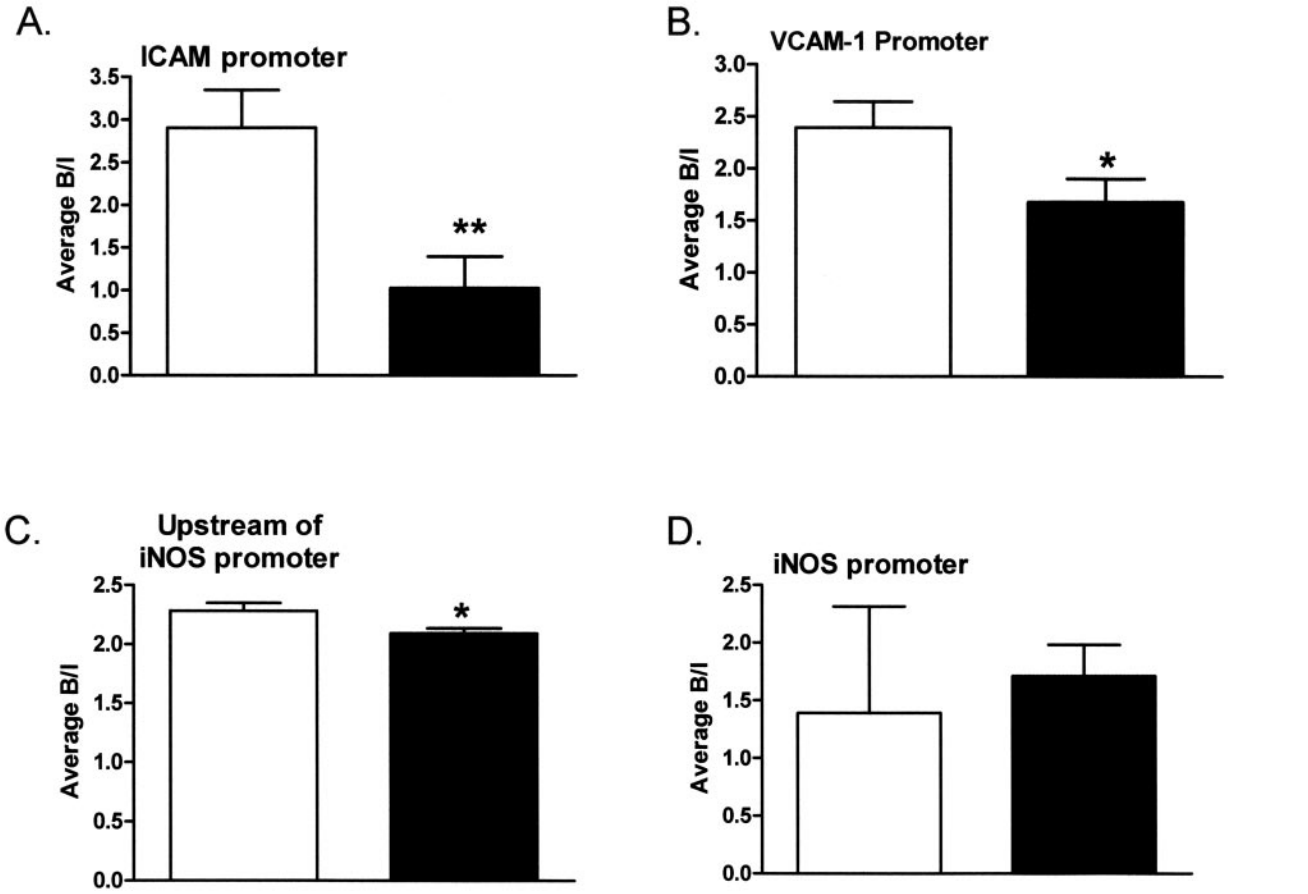

Fig. 6. Effect of TSA on association of histone H1 at local genomic sites using ChIP. MLEC were treated with 0 (□) 0.1 μM trichostatin A (TSA) (■) for 24 h. Cells were processed as in Fig. 5. A, histone H1 associated with the ICAM-1 promoter. B, histone H1 associated with the VCAM-1 promoter. C, histone H1 associated with sequences upstream of the iNOS promoter. D, histone H1 associated with the iNOS promoter. **, $p < 0.005$; *, $p < 0.05$ for comparison between 0 and 0.1 μM TSA.

DNA (Hansen, 2002). In fact, raising acetylation with inhibitors of histone deacetylases causes nuclease hypersensitivity (Simpson, 1978). As expected, inhibition of histone deacetylases with trichostatin A in the present study increased the level of acetyl-histone H3 (Fig. 1B) and enhanced nuclease sensitivity (Fig. 2). Although integrin engagement did not affect poly(ADP-ribosyl)ation, it increased histone H3 acetylation (Fig. 1A) and nuclease sensitivity (Jones et al., 2001). The results suggest that acetylation of histone H3 may contribute to the effect of integrin engagement on chromatin.

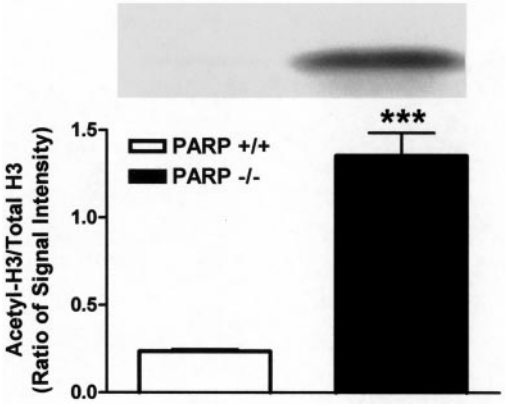

Fig. 7. Acetyl-histone H3 protein levels in wild-type (PARP +/+) and PARP-1 knockout (PARP −/−) MLEC. PARP +/+ (□) and PARP −/− (■) MLEC proteins were extracted and processed for Western blotting. Acetyl-histone H3 was measured by Western blotting and analyzed densitometrically. Blots were also probed with total histone H3 antibody, analyzed, and used to normalize acetyl-histone H3 levels. Bars represent the mean ± S.E. of four independent cultures per treatment group. ***, $p < 0.0002$ for comparison with PARP +/+.

It is interesting that PARP-1 knockouts, which are hypersensitive to nuclease digestion (Jones et al., 2001), were also highly acetylated on histone H3 (Fig. 8). Therefore, acetylation may also contribute to chromatin alterations in these cells. However, deletion of PARP-1 may raise nuclease sensitivity independent of acetylation. In vitro degradation of an oligonucleotide substrate by cellular nucleases was increased in PARP-1-depleted and PARP-1 knockout cell extracts, suggesting that PARP-1 directly protects DNA (Parsons et al., 2005). PARP-1 may also indirectly protect DNA by recruiting DNA binding proteins such as nuclear factor κB (Chang and Alvarez-Gonzalez, 2001), and by association with nucleosomes, which promotes compaction (Kim et al., 2004). Acetylation and the absence of PARP-1 molecules together may produce the nuclease hypersensitivity seen in the knockouts.

Increased histone H3 acetylation in integrin antibody-treated and PARP-1 knockout cells may result from activation of histone acetyl transferases and/or reduction or inhibition of histone deacetylases. With respect to PARP-1, fibroblasts from knockout embryos had decreased expression of a number of histone acetyl transferases, but their activity was not measured (Ota et al., 2003). The activities of histone

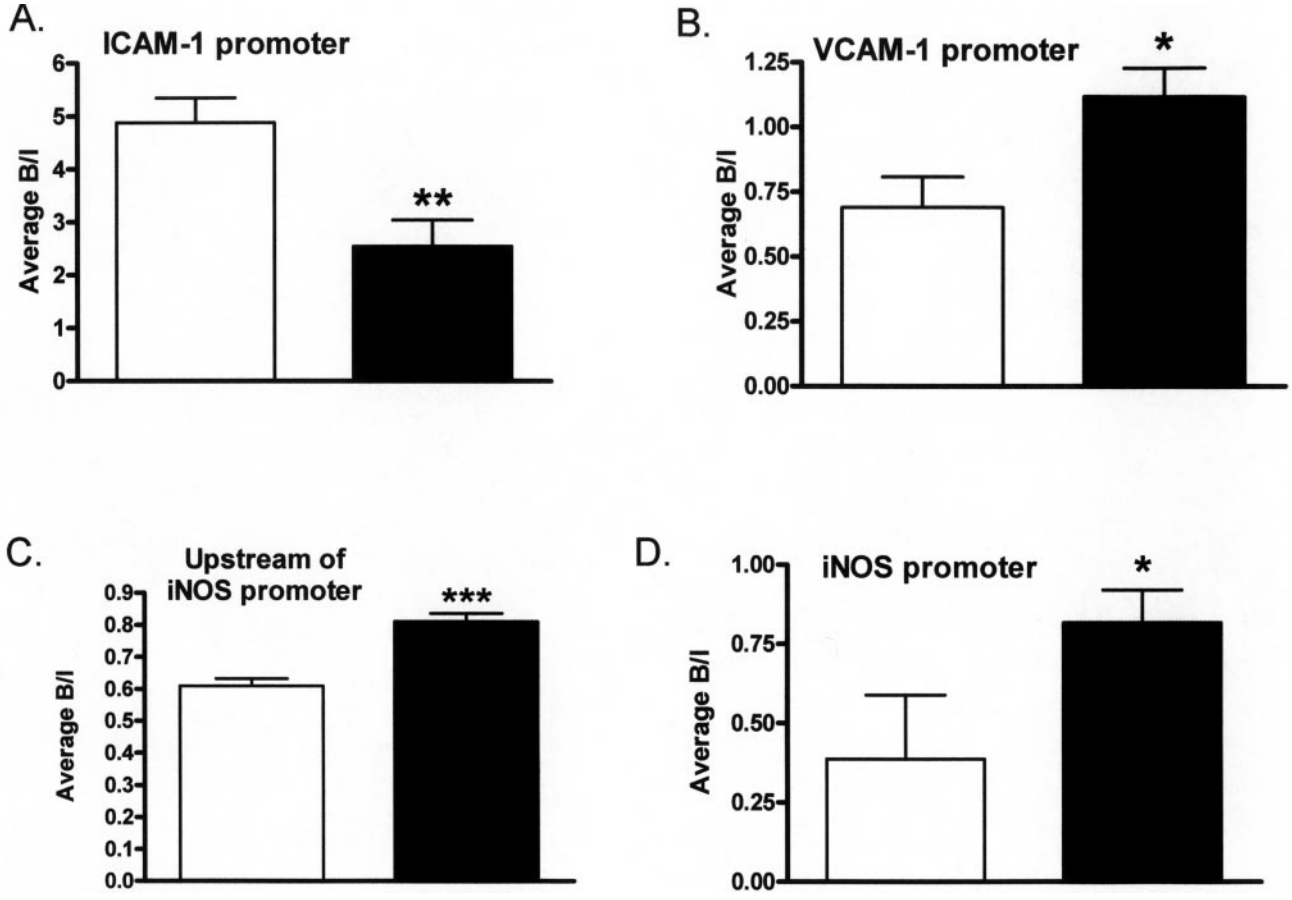

Fig. 8. Effect of PARP-1 on acetyl-Histone H3 immunoprecipitation at local genomic sites using ChIP. PARP +/+ (□) and PARP −/− (■) MLEC were processed as in Fig. 3. A, acetyl-histone H3 coimmunoprecipitated with the ICAM-1 promoter. B, acetyl-histone H3 coimmunoprecipitated with the VCAM-1 promoter. C, acetyl-histone H3 coimmunoprecipitated with sequences upstream of iNOS promoter. D, acetyl-histone H3 coimmunoprecipitated with the iNOS promoter. *, $p < 0.05$; **, $p < 0.001$ and $p < 0.0001$ for comparison between PARP +/+ and PARP −/−.

acetyl transferases and deacetylases need to be assessed in PARP-1 knockout and integrin antibody-treated MLEC. Acetylation may also increase in response to other histone post-translational modifications, such as phosphorylation or ubiquitination, which can affect the susceptibility of histones to acetyl transferases and deacetylases (Berger, 2001).

Having assessed the global chromatin characteristics, we measured histone presence at promoter and nonpromoter DNA to begin examining local variations in DNA-protein interactions in integrin antibody-treated, trichostatin A-treated, and PARP-1 knockout MLEC. Chromatin immunoprecipitation revealed increased relative presence of acetyl-histone H3 at promoter and nonpromoter DNA targets (Figs. 3, 4, and 8). Exceptions to this general trend at the ICAM promoter in PARP-1 knockouts, and the iNOS promoter in trichostatin A-treated and integrin antibody-treated MLEC, suggest that additional factors modulate the presence of acetyl-histone H3 at specific DNA targets. Nevertheless, increases in acetyl-histone H3 are consistent with global nuclease hypersensitivity in these experimental conditions.

Trichostatin A, β1 integrin engagement, and PARP-1 knockout generally reduced the level of linker histone H1 associated at the promoter and nonpromoter DNA targets (Figs. 5, 6, and 9). As an exception, trichostatin A did not reduce histone H1 association with iNOS promoter DNA, suggesting that additional factors affect histone H1 association at particular DNA targets. In any case, reduction in histone H1-DNA association in treated and knockout MLEC is also consistent with global nuclease hypersensitivity.

This study focused on the chromatin structural alterations caused by integrin engagement. The results suggest that acetylation of histone H3 may contribute to the opening of chromatin in response to integrin signals. In several other experimental systems, histone acetylation is associated with enhanced DNA repair (Ramanathan and Smerdon, 1989; Bird et al., 2002; Hasan and Hottiger, 2002; Peterson and Cote, 2004). Whether integrin-mediated acetylation of histone H3 inhibits drug-induced DNA damage or enhances repair remains to be determined.

In summary, integrin engagement, trichostatin A, and PARP-1 knockout increased acetylation of histone H3 and caused nuclease hypersensitivity in MLEC. Consistent with these global effects, the levels of acetyl-histone H3 present at several DNA targets were increased, whereas histone H1 association was generally reduced. The results suggest that integrin engagement, along with trichostatin A and PARP-1 deletion, regulate chromatin structure via core histone H3 acetylation and linker histone H1 dissociation.

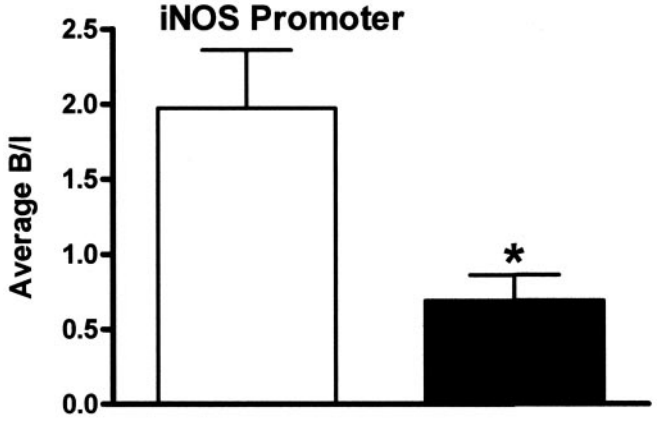

Fig. 9. Effect of PARP-1 on histone H1 association at iNOS promoter using ChIP. PARP +/+ (□) and PARP −/− (■) MLEC were processed as in Fig. 5. Bars represent relative histone H1 associated with the iNOS promoter. *, $p < 0.05$, for comparison between PARP +/+ and PARP −/−.

Acknowledgments

We thank Csaba Szabo (Inotek Corporation, Beverly, MA) for providing PARP-1 knockout mice. The technical assistance of Rostislav I. Likhotvorik is also greatly appreciated.

References

Ame JC, Spenlehauer C, and de Murcia G (2004) The PARP superfamily. *Bioessays* **26:**882–893.
Aplin AE, Howe A, Alahari SK, and Juliano RL (1998) Signal transduction and signal modulation by cell adhesion receptors: the role of integrins, cadherins, immunoglobulin-cell adhesion molecules and selectins. *Pharmacol Rev* **50:**197–263.
Berger SL (2001) An embarrassment of niches: the many covalent modifications of histones in transcriptional regulation. *Oncogene* **20:**3007–3013.
Bird AW, Yu DY, Pray-Grant MG, Qiu Q, Harmon KE, Megee PC, Grant PA, Smith MM, and Christman MF (2002) Acetylation of histone H4 by Esa1 is required for DNA double-strand break repair. *Nature (Lond)* **419:**411–415.
Buckley S, Driscoll B, Barsky L, Weinberg K, Anderson K, and Warburton D (1999) ERK activation protects against DNA damage and apoptosis in hyperoxic rat AEC2. *Am J Physiol* **277:**L159–L156.
Chang WJ and Alvarez-Gonzalez R (2001) The sequence-specific DNA binding of NF-κB is reversibly regulated by the automodification reaction of poly (ADP-ribose) polymerase 1. *J Biol Chem* **276:**47664–47670.
D'Amours D, Desnoyers S, D'Silva I, and Poirier GG (1999) Poly(ADP-ribosyl)ation reactions in the regulation of nuclear functions. *Biochem J* **342:**249–268.
Hansen JC (2002) Conformational dynamics of the chromatin fiber in solution: determinants, mechanisms and functions. *Annu Rev Biophys Biomol Struct* **31:**361–392.
Hasan S and Hottiger MO (2002) Histone acetyl transferases: a role in DNA repair and DNA replication. *J Mol Med* **80:**463–474.
Hazlehurst LA, Valkov N, Wisner L, Storey JA, Boulware D, Sullivan DM, and Dalton WS (2001) Reduction in drug-induced DNA double-strand breaks associated with beta1 integrin-mediated adhesion correlates with drug resistance in U937 cells. *Blood* **98:**1897–1903.
Hewish DR and Burgoyne LA (1973) Chromatin sub-structure. The digestion of chromatin DNA at regularly spaced sites by a nuclear deoxyribonuclease. *Biochem Biophys Res Commun* **52:**504–510.
Hoyt DG, Mannix RJ, Gerritsen ME, Watkins SC, Lazo JS, and Pitt BR (1996a) Integrins inhibit LPS-induced DNA strand breakage in cultured lung endothelial cells. *Am J Physiol* **270:**L689–L694.
Hoyt DG, Rizzo M, Gerritsen ME, Pitt BR, and Lazo JS (1997) Integrin activation protects pulmonary endothelial cells from the genotoxic effects of bleomycin. *Am J Physiol* **273:**L612–L617.
Hoyt DG, Rusnak JM, Mannix RJ, Modzelewski RA, Johnson CS, and Lazo JS (1996b) Integrin activation suppresses etoposide-induced DNA strand breakage in cultured murine tumor-derived endothelial cells. *Cancer Res* **56:**4146–4149.
Huang H, McIntosh JL, Fang L, Szabo C, and Hoyt DG (2003) Integrin-mediated suppression of endotoxin-induced DNA damage in lung endothelial cells is sensitive to poly(ADP-ribose) polymerase-1 gene deletion. *Int J Mol Med* **12:**533–540.
Jones CB, McIntosh J, Huang H, Graytock A, and Hoyt DG (2001) Regulation of bleomycin-induced DNA breakage and chromatin structure in lung endothelial cells by integrins and poly(ADP-ribose) polymerase. *Mol Pharmacol* **59:**69–75.
Kim M, Mauro S, Gévry N, Lis J, and Kraus W (2004) NAD^+-dependent modulation of chromatin structure and transcription by nucleosome binding properties of PARP-1. *Cell* **119:**803–814.
Meredith JE Jr, Fazeli B, and Schwartz MA (1993) The extracellular matrix as a cell survival factor. *Mol Biol Cell* **4:**953–961.
Ota K, Kameoka M, Tanaka Y, Itaya A, and Yoshihara K (2003) Expression of histone acetyltransferases was down-regulated in poly(ADP-ribose) polymerase-1-deficient murine cells. *Biochem Biophys Res Commun* **310:**312–317.
Parsons JL, Dianova II, Allinson SL, and Dianov GL (2005) Poly(ADP-ribose) polymerase-1 protects excessive DNA strand breaks from deterioration during repair in human cell extracts. *FEBS J* **272:**2012–2021.
Perez-Lamigueiro MA and Alvarez-Gonzalez R (2004) Polynucleosomal synthesis of poly(ADP-ribose) causes chromatin unfolding as determined by micrococcal nuclease digestion. *Ann NY Acad Sci* **1030:**593–598.
Peterson CL and Cote J (2004) Cellular machineries for chromosomal DNA repair. *Genes Dev* **18:**602–616.
Ramanathan B and Smerdon MJ (1989) Enhanced DNA repair synthesis in hyperacetylated nucleosomes. *J Biol Chem* **264:**11026–11034.
Realini CA and Althaus FR (1992) Histone shuttling by poly(ADP-ribosylation). *J Biol Chem* **267:**18858–18865.
Simpson RT (1978) Structure of chromatin containing extensively acetylated H3 and H4. *Cell* **13:**691–699.
Snedecor GW and Cochrane WG (1980) *Statistical Methods*, 7th ed, Iowa State University Press, Ames, IA.

Address correspondence to: Dr. Dale G. Hoyt, Division of Pharmacology, The Ohio State University College of Pharmacy, 500 West Twelfth Avenue, Columbus, OH 43210. E-mail: hoyt.27@osu.edu